International Journal of Scientific Research and Engineering Development-– Volume 8 Issue 5, Sep - Oct 2025
Available at www.ijsred.com

RESEARCH ARTICLE OPEN ACCESS

Influence of the Inductance Ratio in the Oscillating Circuit on the Load Characteristics of an LLC Resonant DC-DC Converter

Georgi Petrov Terziyski*
*(Department of Electrical Engineering, Electronics and Automation, University of Food Technologies, Plovdiv, Bulgaria
Email: g_terziyski@uft-plovdiv.bg)
Mariyana Encheva Sestrimska**
**(Department of Electrical Engineering, Electronics and Automation, University of Food Technologies, Plovdiv, Bulgaria
Email: m_sestrimska@uft-plovdiv.bg)
Petio Dimitrov Spasov***
***(Department of Electrical Engineering, Electronics and Automation, University of Food Technologies, Plovdiv, Bulgaria
Email: petio_spasov2001@abv.bg

----------**********----------

Abstract:

This paper presents an LLC resonant DC-DC converter operating at a frequency above the resonant frequency. Based on a study using the first harmonic method, the main dependencies for the currents through the power devices have been determined. The load characteristics of the converter have been constructed. A methodology for its design has been proposed. The influence of the ratio of inductances in the resonant circuit of the resonant converter on the obtained load characteristics has been studied.

Keywords **— LLC resonant DC-DC converter, electrical load diagram, photovoltaic panels**

----------**********----------

I. INTRODUCTION

LLC resonant DC-DC converters are widely used in practice for power supplies of lasers, fluorescent lamps, welding machines, and also in photovoltaic applications [4], [6], [7], [8]. These resonant converters can operate in the entire load range – from no-load to short circuit, which is why they are most often preferred, as they provide maximum efficiency while maintaining the conditions for soft commutation of the inverter power devices [1], [3], [9].

Many authors [4], [6], [7], [8] recommend the use of such converters when connecting them to photovoltaic panels. As a result of the theoretical study of these converters [5], [6], [9], equations for the output and load characteristics were obtained, a methodology for designing the converter was proposed, and the influence of inductances in the oscillating circuit of the resonant converter was studied at different ratios a=3.0 and a=9.0, which are some of the most commonly used in practice.

II. CONVERTER ANALYSIS

The schematic of the LLC resonant DC-DC converter is presented in Fig.1. It is composed of an inverter (managed switches $S_1 \div S_4$ with reverse diodes $D_1 \div D_4$), resonant circuit (L_1, L_2 и C), uncontrollable rectifier ($D_5 \div D_8$), capacitive filter (C_F) and load resistor (R_0). It is assumed that only the first harmonics of the voltages and currents operate in the circuit and all elements in the circuit are ideal (no losses are generated in them), the power devices are switched instantaneously, and the ripples of the supply U_d and output U_0 voltages are negligibly small.

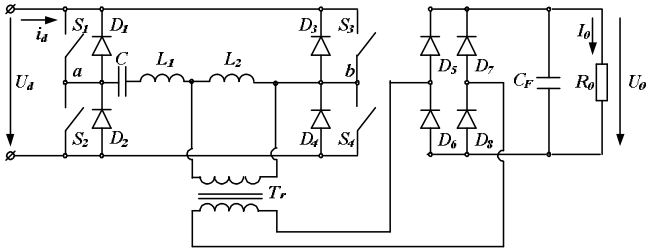

Figure 1. LLC resonant DC-DC converter

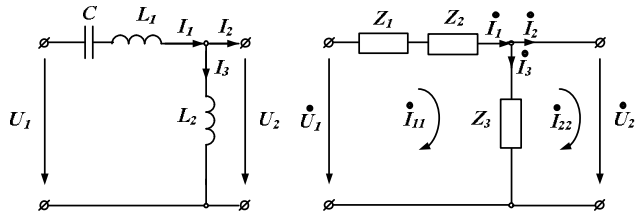

Figure 2. Resonant circuit

In this work the following notations are adopted:

$U_0^{'} = U_0 / U_d$ - normalized output voltage;

$I_0^{'} = I_0 / (U_d / \rho_0)$ - normalized output current;

$I_d^{'} = I_d / (U_d / \rho_0)$ - normalized input current;

$R_0^{'} = R_0 / \rho_0 = U_0^{'} / I_0^{'}$ - normalized load parameter;

$\rho_0 = \sqrt{(L_1 + L_2)/C}$ - characteristic impedance of the oscillating circuit;

$a = L_2 / L_1$ - ratio between the two inductances L_1 and L_2 in the oscillating circuit;

$P_0^{'} = U_0 I_0 / (U_d^2 / \rho_0)$ - normalized output power;

$\nu = \omega_s / \omega_0$ - frequency detuning of the oscillating circuit;

ω_s - converter operating frequency;

$\omega_0 = 1/\sqrt{L_1 C(1+a)}$ - resonant frequency of the oscillating circuit.

When analyzing the essence of the converter, it is assumed that the two circuits of the resonant circuit are equivalent, then according to the method of loop currents, the following system of equations is compiled [2]:

$$\begin{vmatrix} (Z_1 + Z_2 + Z_3)\dot{I}_{11} - Z_3.\dot{I}_{22} = \dot{U}_1 \\ -Z_3.\dot{I}_{11} + Z_3.\dot{I}_{22} = -\dot{U}_2 \end{vmatrix} \quad (1)$$

After formal transformations, the following expression for the voltage $\dot{U}_2$ is obtained:

$$\dot{U}_2 = \frac{\dot{U}_1.Z_3 - Z_1 Z_3.\dot{I}_{22} - Z_2 Z_3.\dot{I}_{22}}{Z_1 + Z_2 + Z_3} \quad (2)$$

The impedances of the coils and the capacitor of the resonant circuit should be replaced with their equivalent equations:

$$\begin{aligned} Z_1 &= 1/j\omega C = \rho_0 / j.\nu; \\ Z_2 &= j\omega L_1 = j.\nu.\rho_0; \\ Z_3 &= j\omega L_2 = a.Z_2 = j.\nu.\rho_0.a. \end{aligned} \quad (3)$$

After substituting the impedances (3) into formula (2) and some mathematical transformations, we obtain:

$$\dot{U}_2 = \frac{\dot{U}_1.\nu^2.a.(1+a)}{(\nu^2.a+\nu^2-a-1).(1+a)} + j\frac{\nu.\rho_0.a.(1+a-\nu^2).\dot{I}_{22}}{(\nu^2.a+\nu^2-a-1).(1+a)} \quad (4)$$

The vector diagram of the voltages from the resonant circuit has the following form:

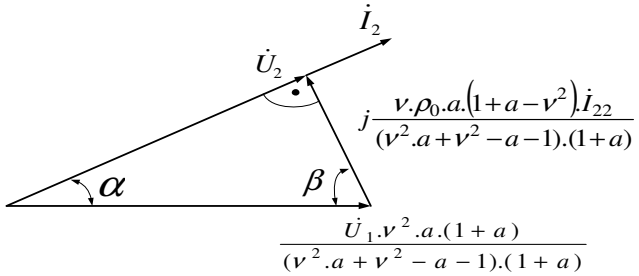

Figure 3. Vector diagram of voltages

For the resulting vector diagram (in the form of a right triangle) the Pythagorean theorem is valid:

$$\dot{U}_2^2 + \left[\frac{\nu.\rho_0.a.(1+a-\nu^2).\dot{I}_{22}}{(\nu^2.a+\nu^2-a-1).(1+a)}\right]^2 = \left[\frac{\dot{U}_1.\nu^2.a.(1+a)}{(\nu^2.a+\nu^2-a-1).(1+a)}\right]^2 \quad (5)$$

After some modifications, it is obtained:

$$\dot{U}_2^2.(\nu^2.a+\nu^2-a-1)^2.(1+a)^2 + \nu^2.\rho_0^2.a^2.(1+a-\nu^2)^2.\dot{I}_{22}^2 = \dot{U}_1^2.\nu^4.a^2.(1+a)^2 \quad (6)$$

where:

$$\begin{aligned} \dot{U}_1 &= \frac{2.\sqrt{2}}{\pi}.U_d \\ \dot{I}_{22} &= \frac{\pi}{2.\sqrt{2}}.I_0 \\ \dot{U}_2 &= \frac{2.\sqrt{2}}{\pi}.U_0 \end{aligned} \quad (7)$$

By substituting the dependencies (7) into (6) in relative units, the expression is obtained:

$$U_0^{'} = \sqrt{\frac{\nu^4.a^2.(1+a)^2 - \frac{\pi^4}{64}.\nu^2.a^2.(1+a-\nu^2)^2.I_0^{'2}}{(\nu^2.a+\nu^2-a-1)^2.(1+a)^2}} \quad (8)$$

The last expression (8) defines the equation of the desired output characteristics $U_0^{'} = f(I_0^{'}, \nu, a)$.

From equation (8) the equation for the regulation characteristics can be obtained, for which purpose the output current I_0 is expressed in terms of the output voltage U_0 and the load resistance R_0. As a result, the equation is obtained:

$$U_0^{'}=\frac{8.\nu.a.R_0^{'}.(1+a)}{\sqrt{64.R_0^{'2}.(\nu^2.a+\nu^2-a-1)^2.(1+a)^2+\pi^4.\nu^2.a^2.(1+a-\nu^2)^2}}, \quad (9)$$

where $R_0^{'}$ is a normalized value for the resistance of the load resistor.

The output power of the converter in relative units can be expressed from the equation for the output characteristics, after its multiplication by $I_0^{'}$:

$$P_0^{'}=\frac{I_0^{'}}{8.(\nu^2.a+\nu^2-a-1).(1+a)}.\sqrt{64.\nu^4.a^2.(1+a)^2-\pi^4.\nu^2.a^2.(1+a-\nu^2)^2.I_0^{'2}} \quad (10)$$

At a set value of ν the function $P_0^{'}=f(I_0^{'},\nu,a)$ has a maximum at:

$$U_0^{'}=\frac{\nu^2.a}{4\sqrt{2}.(\nu^2.a+\nu^2-a-1)} \text{ и } I_0^{'}=\frac{4\sqrt{2}.\nu.(1+a)}{\pi^2.(1+a-\nu^2)} \quad (11)$$

$$P_{0\max}^{'}=\frac{\nu^3.a.(1+a)}{\pi^2.(\nu^2.a+\nu^2-a-1).(1+a-\nu^2)} \quad (12)$$

The relative resistance of the resistor in which the maximum power is dissipated is:

$$R_{0\max}^{'}=\frac{\pi^2.\nu.a.(1+a-\nu^2)}{32.(\nu^2.a+\nu^2-a-1).(1+a)} \quad (13)$$

For the effective value of the current through the coil of the resonant circuit, the expression is obtained:

$$I_1^{'}=\sqrt{\frac{\pi^4.\nu^2.a^2.I_0^{'2}+64.(1+a)^2.U_0^{'2}}{8.\pi^2.\nu^2.a^2}} \quad (14)$$

The average values of the currents through the rectifier diodes are determined based on the output current, taking into account that each of them conducts one half-cycle:

$$I_{D\_RECT\,AV}^{'}=\frac{I_0^{'}}{2} \quad (15)$$

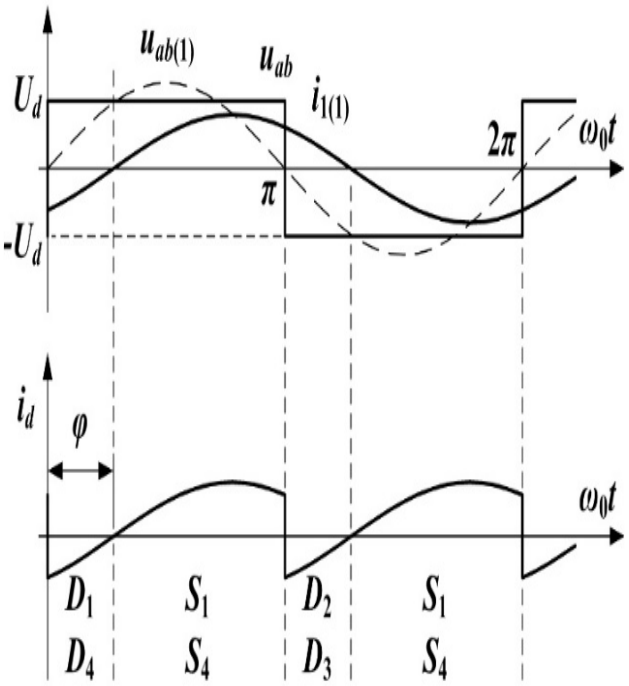

Figure 4. Waveforms of the inverter voltages and current

From the above it follows that the normalized average values of the currents through the controlled switches are determined as follows:

$$I_{S\,AV}^{'}=\frac{1}{2\pi}\int_0^{\pi-\varphi}\sqrt{2}I_1^{'}\sin\omega t d\omega t=\frac{\sqrt{2}}{2\pi}I_1^{'}(1+\cos\varphi) \quad (16)$$

Similarly for the currents through the antiparallel diodes we get:

$$I_{DAV}^{'}=\frac{1}{2\pi}\int_{\pi-\varphi}^{\pi}\sqrt{2}I_1^{'}\sin\omega t d\omega t=\frac{\sqrt{2}}{2\pi}I_1^{'}(1-\cos\varphi) \quad (17)$$

Then the normalized average value of the current consumed by the power source is:

$$I_{d\,AV}^{'}=\frac{1}{\pi}\int_0^{\pi}\sqrt{2}I_1^{'}\sin(\omega t-\varphi)d\omega t=\frac{2\sqrt{2}}{\pi}I_1^{'}\cos\varphi \quad (18)$$

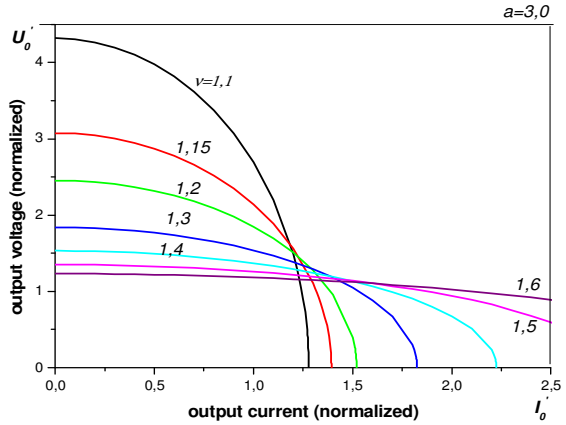

Figure 5. Dependences of converter voltage on output current

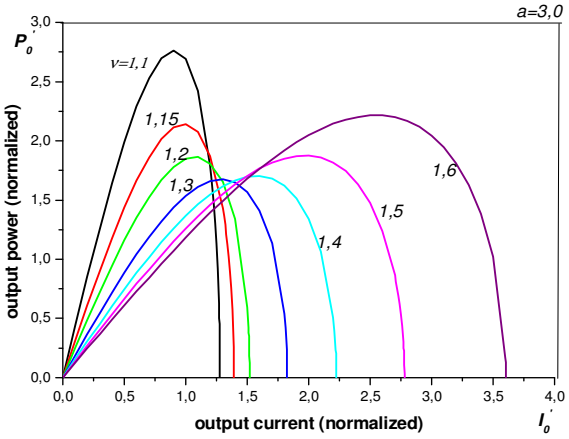

Figure 6. Dependences of converter power on output current

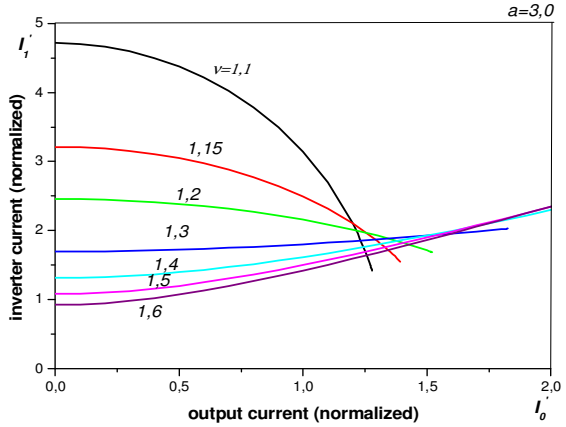

Figure 7. Dependences of converter current on output current

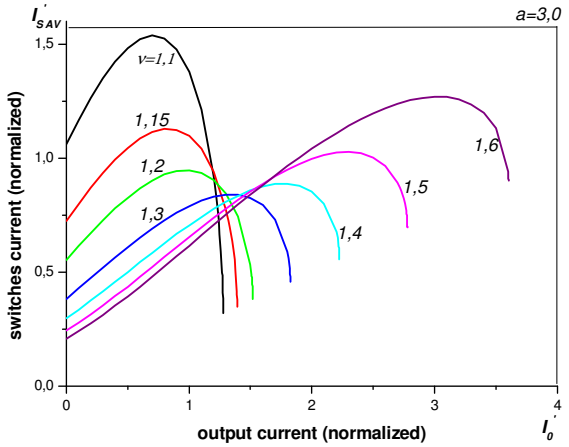

Figure 8. Dependences of the average values of the currents through the controlled switches on the output current

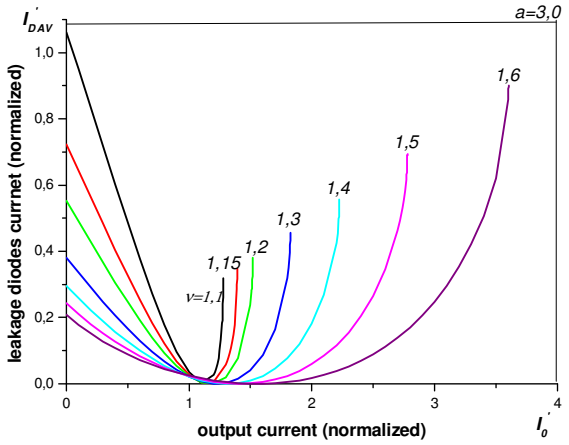

Figure 9. Dependences of the average values of the currents through the reverse diodes on the output current

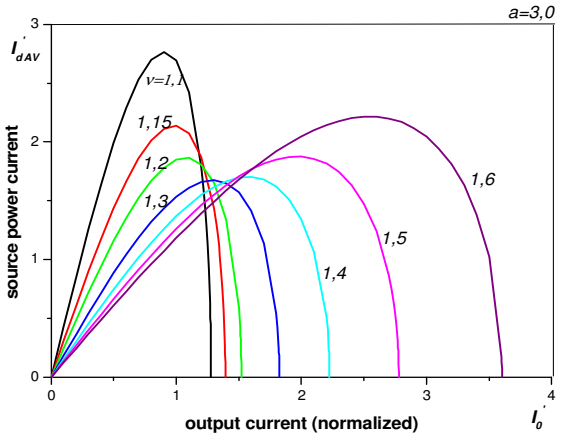

Figure 10. Dependencies of the average values of the current consumed by the power source

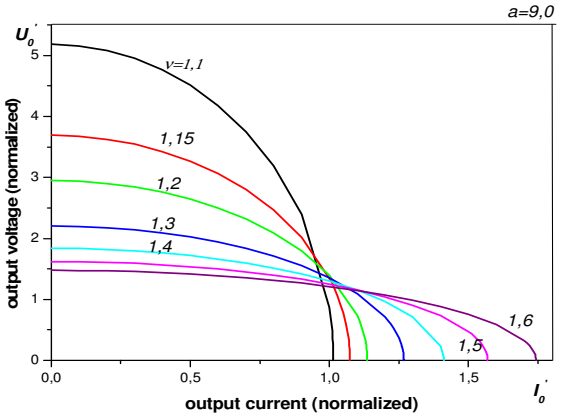

Figure 11. Dependences of converter voltage on output current

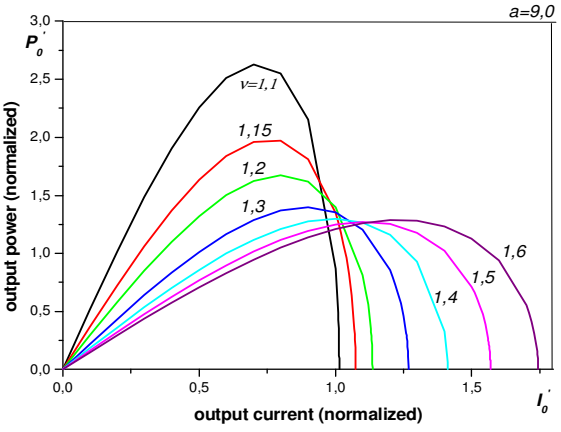

Figure 12. Dependences of converter power on output current

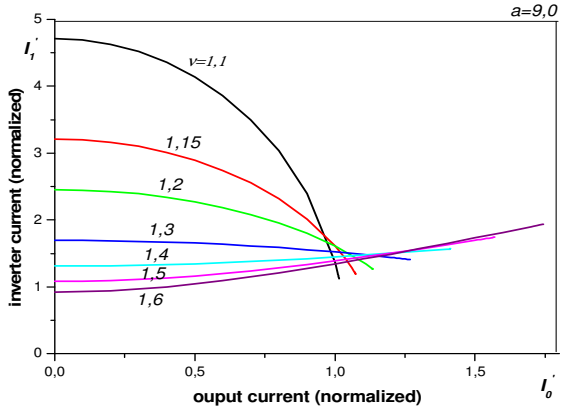

Figure 13. Dependences of converter current on output current

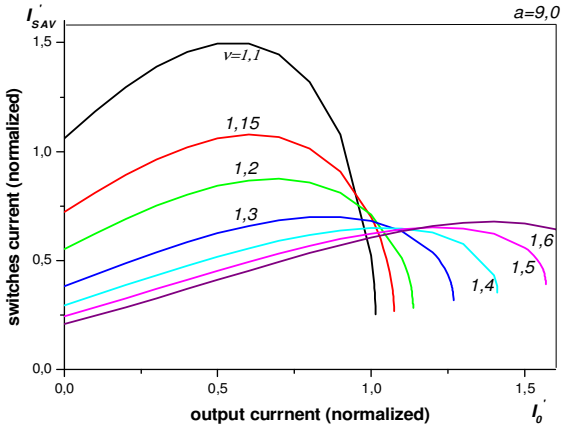

Figure 14. Dependences of the average values of the currents through the controlled switches on the output current

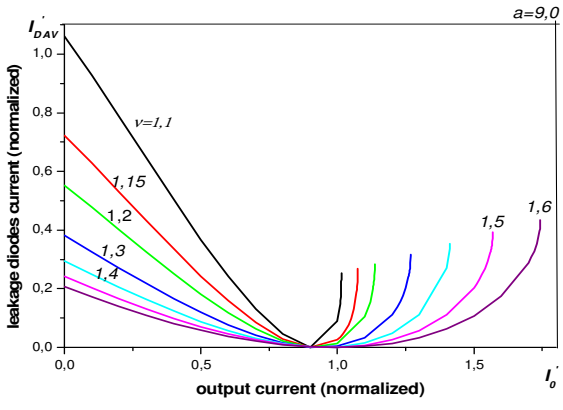

Figure 15. Dependences of the average values of the currents through the reverse diodes on the output current

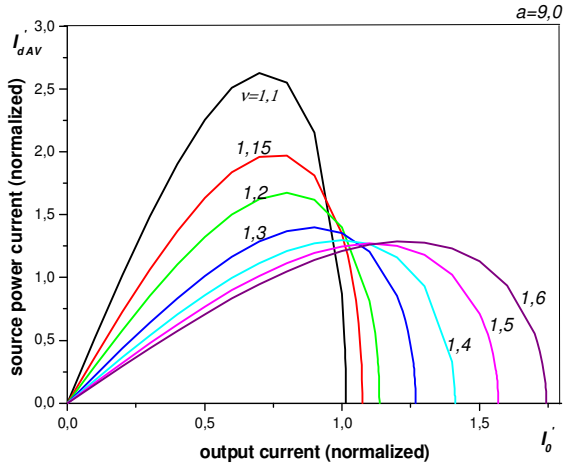

Figure 16. Dependencies of the average values of the current consumed by the power source

The output characteristics presented in Fig. 5 and Fig. 9 make it clear that when the converter is operated above its resonant frequency with increasing operating frequency, the short-circuit current increases and the open-circuit voltage decreases. Also, the characteristics intersect and are inherent to a current-limited voltage source. In addition, it is seen that the open-circuit voltage and short-circuit current are different at a=3.0 and a=9.0, and the same applies to the other characteristics demonstrated in Figures 10÷16.

The obtained characteristics for the output power of the studied converter are given in Fig. 6 and Fig. 12 and show that when the converter operates above its resonant frequency $\nu = 1{,}1 - 1{,}3$ with increasing operating frequency, the short-circuit current increases, and the output power decreases to frequency detuning $\nu = 1{,}3$. When increasing ν above 1.3, it is seen that the output power increases with increasing short-circuit current.

Based on equation (14), Fig. 7 and Fig. 13 present normalized dependences of the converter current on the output current, obtained for the parameter a=3.0 and a=9.0 and different values of the frequency detuning $\nu > 1{,}0$. Identical in shape characteristics are obtained with a clearly pronounced maximum, which with an increase in the frequency detuning shifts to the end of the coordinate system. In addition, the converter current always has a value other than zero for the entire range of load changes. Moreover, with frequency detuning $\nu = 1{,}1$, the current through the converter can have a significant value, even with a small output current. Therefore, in this case, significant losses will also be observed in the studied converter.

Based on equation (16) in Fig. 8 and Fig. 14 are demonstrated the normalized functions of the average values of the currents through the controlled switches of the inverter from the output current, obtained at a=3.0 and a=9.0 for different values of the frequency tuning $\nu > 1{,}0$. From the characteristics it is seen that the average values of the currents through the controlled switches for the entire load range have non-zero values. On the other hand from $\nu = 1{,}1$, at the average value of the current through the controlled switches can be significant, thus increasing the losses.

Based on equation (17), Fig. 9 and Fig. 15 show normalized dependences of the average values of the currents through the inverter's reverse diodes on the output current, obtained at a=3.0 and a=9.0 at different values of the frequency tuning $\nu > 1{,}0$. The figures show that with increasing frequency detuning $\nu = 1{,}1 \div 1{,}6$ the characteristics become similar and have a minimum, which with increasing frequency detuning is shifted towards the end of the coordinate system. In addition, the current through the inverter's reverse diodes always has a non-zero value for the entire range of load changes. Moreover, with frequency detuning $\nu = 1{,}6$ the current through the inverter's reverse diodes can have a significant value, even with a small output current.

Based on equation (18), Fig. 10 and Fig. 16 show normalized dependences of the average values of the current consumed by the power source, obtained at a=3.0 and a=9.0 at different values of the frequency detuning $\nu > 1{,}0$. The characteristics show that with increasing operating frequency $\nu = 1{,}1 \div 1{,}3$, the short-circuit current increases, and the current consumed by the power source decreases. With increasing operating frequency for $\nu = 1{,}4 \div 1{,}6$, the

short-circuit current and the current consumed by the power source increase.

III. DESIGN OF LLC RESONANT DC-DC CONVERTER

When designing the considered resonant DC-DC converter, the following parameters are usually set: output power P_0, output voltage U_0 and operating frequency f. If it is assumed that the efficiency coefficient of the inverter is equal to unity, the parameters of the power source are:

$$U_d = \frac{U_0}{U_0'} = \frac{U_0}{\sqrt{\frac{\nu^4.a^2.(1+a)^2 - \frac{\pi^4}{64}.\nu^2.a^2.(1+a-\nu^2)^2.I_0'^2}{(\nu^2.a+\nu^2-a-1)^2.(1+a)^2}}} \quad (19)$$

$$I_d = \frac{P_0}{U_d} = \frac{P_0.\sqrt{\frac{\nu^4.a^2.(1+a)^2 - \frac{\pi^4}{64}.\nu^2.a^2.(1+a-\nu^2)^2.I_0'^2}{(\nu^2.a+\nu^2-a-1)^2.(1+a)^2}}}{U_0} \quad (20)$$

The values of the switching elements L_1, C and L_2 are determined by the expressions for the maximum output power and the detuning of the resonant circuit:

$$P_0 = \frac{\nu^3.a.(1+a)}{\pi^2.(\nu^2.a+\nu^2-a-1).(1+a-\nu^2)}.\frac{U_d^2}{\sqrt{\frac{L_1.(1+a)}{C}}} \quad (21)$$

$$\nu = 2.\pi.f.\sqrt{L_1.C.(1+a)} \quad (22)$$

Then for L_1, C and L_2 the following dependencies are obtained:

$$L_1 = \frac{\nu^4.a}{2\pi^3.(\nu^2.a+\nu^2-a-1).(1+a-\nu^2)}.\frac{U_d^2}{f.P_0} \quad (23)$$

$$C = \frac{\pi.(\nu^2.a+\nu^2-a-1).(1+a-\nu^2)}{2\nu^2.a.(1+a)}.\frac{P_0}{f.U_d^2} \quad (24)$$

$$L_2 = a.L_1 = \frac{\nu^4.a^2}{2\pi^3.(\nu^2.a+\nu^2-a-1).(1+a-\nu^2)}.\frac{U_d^2}{f.P_0} \quad (25)$$

IV.CONCLUSION

In this article, a study of an LLC resonant DC-DC converter using the first harmonic method, operating at frequencies above the resonant frequency, has been carried out. Based on this study, the main dependencies for the currents through the power devices of the inverter have been determined. The load characteristics of the converter have been constructed and a methodology for its design has been proposed. The influence of the ratio of the two inductances in the resonant converter's oscillating circuit has been studied at ratios a=3.0 and a=9.0, which are some of the most commonly used ratios in practice.

REFERENCES

[1] Azura N., S. Iqbal, S. Taib (2014). LLC Resonant DC-DC Converter for High Voltage Applications, *IEEE*, 90-95.

[2] Batarseh I., Resonant Converter Topologies with Three and Four Energy Storage Elements (1994). *IEEE Transactions on Power Electronics*, 9(1), 64 – 73.

[3] Buccella C., C. Cecati, H. Latafat et al. (2012). Digital Control of a Half-Bridge LLC Resonant Converter, *15th International Power Electronics and Motion Control Conference*, 1-6.

[4] Costa V., M. Perdigao, A. Mendes et al. (2017). Analysis AND Simulation of a LLC-VI Resonat Converter for Solar Application, *IEEE*.

[5] Grigirova Ts., A. Vuchev, I. Maradzhiev (2019). Investigation of an LLC resonant DC/DC converter with a capacitive output filter, Part II – Design Considerations, *Proc. XXVIII International Scientific Conference Electronics – ET2019*, Sozopol, Bulgaria.

[6] Meghana M., S. Naveenkumar (2017). MPPT based LLC Resonant Converter for PV Applications, *International Conference on Computation of Power, Energy, Information and Communication*.

[7] Pandey P., P. Agnihotri (2019). An Efficient LLC Resonant Converter Design for Photovoltaic Application, *IEEE*.

[8] Ragab A., N. Saad, A. El-Sattar (2017). LLC Resonant DC-DC Converter for Grid-Connected PV System, *IEEE*.
[9] Vuchev A., Ts. Grigorova, I. Maradzhiev (2019), Investigation of an LLC resonant DC/DC converter with a capacitive output filter, Part I – Load Characteristics, *Proc. XXVIII International Scientific Conference Electronics – ET2019*, Sozopol, Bulgaria.
[10] Zeng J., G. Zhang, S. Yu et al. (2020). LLC Resonant Converter Topologies and Industrial Application – A Review, *Chinese Journal of Electrical Engineering*, 6 (3).

